

# NUCLEOSYNTHETIC AND COSMOGENIC PALLADIUM ISOTOPE ANOMALIES RESOLVED IN IVB IRONS.

N. Wittig<sup>1,2</sup>, M. Humayun<sup>1</sup> and I. Leya<sup>3</sup> <sup>1</sup>National High Magnetic Field Laboratory & Dept. of Earth, Ocean & Atmospheric Science, Florida State University, Tallahassee, FL 32310, USA ([wittig@magnet.fsu.edu](mailto:wittig@magnet.fsu.edu), [humayun@magnet.fsu.edu](mailto:humayun@magnet.fsu.edu)), <sup>2</sup>Department of Earth Sciences, Carleton University, 1125 Colonel By Drive, Ottawa, Ontario, Canada K1S5B6, <sup>3</sup>Physical Institute, Space Science and Planetology, University of Bern, Sidlerstrasse 5, 3012 Bern, Switzerland.

**Introduction:** Recent Mo [1], Ru [2;3] and W [4-8] isotope studies highlighted the presence of small nucleosynthetic isotope anomalies recorded in meteoritic material, particularly in magmatically fractionated planetary cores such as IVB irons. In contrast, isotope anomalies recorded in Os isotopes are inconsistent with the s-deficit/p,r-excess nucleosynthetic anomalies and clearly result from the galactic cosmic ray (GCR) neutron capture on <sup>189</sup>Os, inducing coupled negative ( $\epsilon^{189}\text{Os}$ ) and positive ( $\epsilon^{190}\text{Os}$ ) effects [8;9]. The origin of the nucleosynthetic effects in Mo, Ru and W are not well understood, but large Mo/Ru isotope anomalies are carried by SiC [10], so that inhomogeneous distribution of presolar grains could induce nucleosynthetic anomalies. Incomplete dissolution of presolar grains has been documented in chondrites [11;12], but is not a plausible cause for nucleosynthetic anomalies in iron meteorites. CAIs show endemic nucleosynthetic anomalies [13], so that an excess of CAIs (refractory element enrichment) in the protoplanets from which iron meteorites were derived can induce s-process deficiencies in refractory elements (Mo, Ru, W and Os), but should not affect the isotopic compositions of non-refractory elements. To test this later idea and to better constrain cosmogenic effects we examined the isotopic composition of Pd in IVB irons, the group that consistently exhibits the largest nucleosynthetic and cosmogenic effects. While Pd is siderophile during magmatic differentiation and partitions into planetesimal cores, it is not a refractory element in contrast to W, Ru and Mo. Pd has six isotopes; the low abundance <sup>102</sup>Pd (1%) and the s-only <sup>104</sup>Pd (11%) in addition to <sup>105</sup>Pd (22%), <sup>106</sup>Pd (27%), <sup>108</sup>Pd (26%) and <sup>110</sup>Pd (12%). Notably, <sup>104</sup>Pd accumulates from neutron capture during GCR burning of <sup>103</sup>Rh, a nuclide with a high neutron capture cross section [14]. We have recently reported correlated cosmogenic anomalies in Pt, Os and W isotopes in IVB irons. Here we present new and highly precise Pd isotope data from the same aliquots [8] and examine the IVB Pd isotopic signatures for inherent nucleosynthetic anomalies predicted from Ru and Mo isotopes, and the extent of GCR-induced neutron capture on <sup>103</sup>Rh, <sup>108</sup>Pd and <sup>109</sup>Ag.

**Analytical Methodology:** Digestion and chemical separation procedures used are identical to [8] and Pd is collected together with Pt. The Pd-Pt cuts yielded from cation and anion exchange column procedures

remove 99.999% of the iron matrix (Fe, Ni, Co, Cu) and potentially interfering trace elements (Zr, Mo, Ru, Cd, Ga etc.), although traces of V, Cr (e.g. Hoba, Weaver Mountains) and Zn can be found in individual samples (e.g. Hoba, Weaver Mountains, Skookum, Tinnie). Pd isotope measurements (92 replicates) were undertaken during 5 analytical sessions on the NHMFL Thermo Neptune™ MC-ICP-MS (Tallahassee) on 100 ng/mL aliquots in 2% HCl to accommodate the low abundance of <sup>102</sup>Pd. An ESI Apex™ introduction system and Thermo SuperJet8.3 Ni sampler and Spectron T1001Ni-X skimmer cones yielded a total Pd signal of 550 V/ppm. The Pd isotope data are normalized to <sup>108</sup>Pd and <sup>105</sup>Pd/<sup>108</sup>Pd = 0.843915 was used for mass bias corrections (exponential law). We report data as  $\epsilon^{102}\text{Pd}$ ,  $\epsilon^{104}\text{Pd}$ ,  $\epsilon^{106}\text{Pd}$  and  $\epsilon^{110}\text{Pd}$ . Inorganic Ventures™ Pd concentration standard (100ng/mL, n= 240, "INVENT") serves as terrestrial bracketing reference material. The typical INVENT within-session reproducibility (2 $\sigma$ ) for  $\epsilon^{102}\text{Pd}$ ,  $\epsilon^{104}\text{Pd}$ ,  $\epsilon^{106}\text{Pd}$  and  $\epsilon^{110}\text{Pd}$  is < 0.45 $\epsilon$ , <0.15 $\epsilon$ , <0.1 $\epsilon$  and <0.2 $\epsilon$ , respectively. Atomic isobaric interferences from Ru and Cd isotopes were negligible as IVB <sup>101</sup>Ru/<sup>108</sup>Pd (<0.000002) and <sup>111</sup>Cd/<sup>108</sup>Pd (<0.000006) were indistinguishable from the pure Pd INVENT standards. Mass 110 appears suffers from an unknown interference in some samples (e.g. Hoba), which could not be fully removed during the purification procedures.

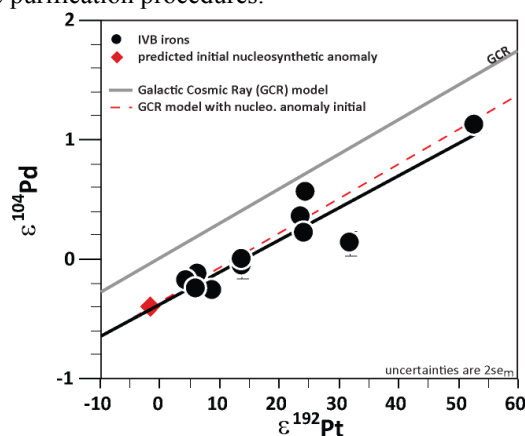


**Fig. 1.** IVB  $\epsilon^{104}\text{Pd}$  vs  $\epsilon^{192}\text{Pt}$  with a linear regression (black line), a GCR neutron capture model (grey) using parameters similar to those detailed in [8] and references therein, a prediction of initial nucleosynthetic Pd and Pt isotope anomalies (red diamond) and the evolution with increasing GCR damage (red dashed line).

**Results:** While  $\epsilon^{102}\text{Pd}$  (-0.25 to +0.10) and  $\epsilon^{106}\text{Pd}$  (-0.15 to +0.29) are not resolved from the terrestrial standard,  $\epsilon^{104}\text{Pd}$  and  $\epsilon^{110}\text{Pd}$  (+0.35 to +1.82) display isotope anomalies distinct from INVENT. The effects in  $\epsilon^{104}\text{Pd}$  are well-correlated with  $\epsilon^{192}\text{Pt}$  (Fig. 1) due to neutron capture effects on  $^{103}\text{Rh}$  and  $^{191}\text{Ir}$ . Tlacotepec, which carries the strongest GCR neutron capture signature in  $\epsilon^{189}\text{Os}$ ,  $\epsilon^{192}\text{Pt}$  and  $\epsilon^{182}\text{W}$  shows the highest  $\epsilon^{104}\text{Pd}$  of +1.12. IVBs with the lowest GCR damage (Weaver Mountains, Warburton Range, Tawallah Valley, Tinnie, Skookum [8]) have resolved negative  $\epsilon^{104}\text{Pd}$  of  $-0.21 \pm 0.15$ . Importantly, the initial  $\epsilon^{104}\text{Pd}$  of IVB irons is distinctly negative at  $-0.35 \pm 0.15$ , which is consistent with a nucleosynthetic effect. The anomalies reported here are smaller than the errors reported on the earlier P-TIMS measurements, including some IVB irons [15]. An anomaly in  $\epsilon^{105,108}\text{Pd}$  reported only in Warburton Range was not duplicated here [14].

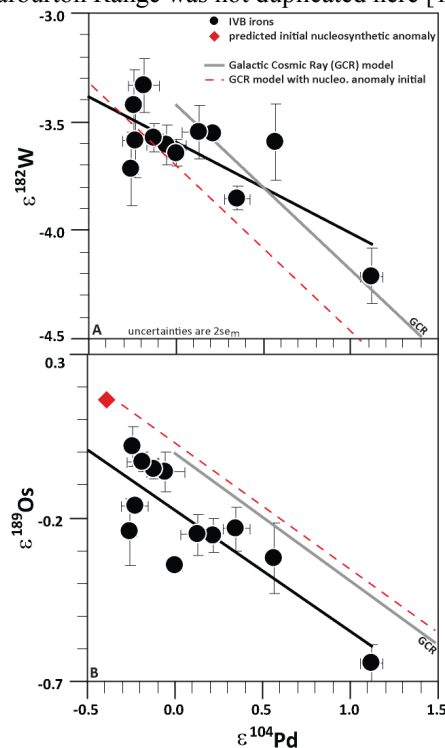


**Fig. 2.** IVB  $\epsilon^{182}\text{W}$  (A) &  $\epsilon^{189}\text{Os}$  (B) vs  $\epsilon^{104}\text{Pd}$ . Symbols as Fig. 1

**Discussion:** Neutron capture cross sections of Mo and Ru isotope are small relative to those of  $^{103}\text{Rh}$  and GCR damage is negligible [1,2,16]. Hence Mo and Ru nucleosynthetic anomalies stem from either s-process deficits (i.e., under-representation of the s-process isotopes  $^{100}\text{Ru}$  and  $^{96}\text{Mo}$ ) or r- (supernovae) and p-processes excesses on other Ru and Mo isotopes [1,2]. Using the s-process abundances of [17], we predict  $\epsilon^{104}\text{Pd}$  and  $\epsilon^{192}\text{Pt}$  deficits of -0.40  $\epsilon\text{u}$  and -1.6  $\epsilon\text{u}$  (Fig. 1), respectively, if IVB Pd-Pt isotopes record the same s-process deficit/r-process excess observed in Mo [1].

A first order observation is that  $\epsilon^{104}\text{Pd}$  correlates well with  $\epsilon^{192}\text{Pt}$ ,  $\epsilon^{189}\text{Os}$  and  $\epsilon^{182}\text{W}$  (Fig. 1,2), highlighting the ubiquitous secondary neutron capture reactions recorded in IVB irons, which obscure initial nucleosynthetic isotope anomalies in Pt. The  $\epsilon^{104}\text{Pd}$ - $\epsilon^{192}\text{Pt}$  correlation yields an initial  $\epsilon^{104}\text{Pd}$  isotope anomaly of  $-0.37 \pm 0.15$  at  $\epsilon^{192}\text{Pt} = 0$ , which is identical to the magnitude predicted (Fig. 1) from Mo nucleosynthetic isotope anomalies. All IVB irons have positive but variable  $\epsilon^{110}\text{Pd}$ , distinct from the predicted positive nucleosynthetic anomaly (+0.4 $\epsilon$ ). This  $\epsilon^{110}\text{Pd}$  range cannot be ascribed to GCR burning of  $^{109}\text{Ag}$ , due to the low abundance of Ag in IVB irons [18] and an analytical artefact has to be considered for the high  $\epsilon^{110}\text{Pd}$  samples.

Our multi-isotope approach resolves the intricate relationship of nucleosynthetic anomalies and GCR neutron capture reactions that govern the W-Os-Pt-Pd isotope systematics in IVB irons and highlights the need for statistically relevant sampling of any meteorite group if meaningful data pertinent to the early solar system evolution is to be extracted from these samples. Further, we may place restrictions on the processes that could induce W, Ru, Mo (strongly to moderately refractory) and Pd (similar to Fe-Co-Ni) nucleosynthetic isotope anomalies while the complementary effects are absent in Os isotopes. Carbon-rich condensates (SiC) have been shown to be carriers of W, Mo and Ru nucleosynthetic anomalies [10]. Pd is not known to form carbides, but since  $\epsilon^{104}\text{Pd}$  exhibits a well-resolved nucleosynthetic anomaly (s-process deficit) this renders phases such as SiC unlikely as the sole origin of these anomalies in IVB iron meteorites.

**References:** [1] Burkhard, C. et al. (2011) *EPSL*, 312, 390-400. [2] Chen, N. et al. (2010) *GCA*, 74, 3815-3862. [3] Fischer-Gödde, M. et al. (2012) *43<sup>rd</sup> LPSC*, #2492. [4] Markowski, A. et al. (2006) *EPSL*, 250, 104-115. [5] Markowski, A. et al. (2006) *EPSL*, 242, 1-15. [6] Qin L. et al. (2008) *EPSL*, 273, 94-104. [7] Schersten, A. et al. (2006) *EPSL*, 241, 530-542. [8] Wittig, N. et al. (2013) *EPSL*, in press. [9] Walker, R.J. (2012) *EPSL*, 315-352, 36-44. [10] Nicolussi, G. et al. (1998) *Astrophys J*, 504, 492-499. [11] Brandon, A. et al. (2005) *Science*, 309, 1233-1236. [12] Yokoyama, T. et al. (2010) *EPSL*, 291, 48-59. [13] Brennecka, G. et al. (2012) *43<sup>rd</sup> LPSC*, #2006. [14] Humayun, M. and Huang, S. (2008) *39<sup>th</sup> LPSC*, #1831. [15] Chen J. H. and Wasserburg G. J. (2005) *36<sup>th</sup> LPSC*, #1495. [16] Mughabhab, S.F. (2013) *IAEA*, 1-31. [17] Arlandini, C. et al. (1999) *Astrophys J*, 525, 886-900. [18] Chen J. H. and Wasserburg G. J. (1996) *AGU Monograph*, 95, 1-20.